2D Finite Element Simulation of Steady-State Groundwater Flow Using MATLAB

Marwa Suliman Omer and Abdelrahman ELzubier Mohamed

Abstract

In this paper, we try to obtain a numerical solution for finite element which is formulated for steady-state groundwater flow discretized by using triangular element grid. Then, a MATLAB program is deveoped for this purpose to get primarily the unknown potential function at the triangular elements nodes. The Simulation of Finite element Field problems MATLAB Program was developed and implemented, as a check and test of nodal potential value. The program SFFP was applied for solution of a two-dimensional porous medium problem, fluid flow problem, and body exposure to a heat source problem. In the meantime, results obtained when compared with published data, found very close with maximum percentage difference of 0.22%. Thus, SFFP was applied to groundwater flow beneath a coffer dam problem of known results as a case study; for verification, a comparison of the results was obtained with a maximum percentage difference of 1.32%. This verifies the accuracy of SFFP results.

Keywords

Potential formulation • Quasi-harmonic equation • Steady-state flow

1 Introduction

As stated by Hinton and Owen (1979) finite element field problem is the situation in which only one degree of freedom exists at each nodal point. In particular, the so-called quasi-harmonic equation which has wide applicability in many branches of engineering and physics is considered. In this way, a finite element program which is developed to solve the two-dimensional quasi-harmonic equation system can be employed to analyze several problems of engineering interest. According to Zienkiewicz et al. (2013) examples of field problems, such as heat conduction, groundwater potential, torsion of shafts, seepage, lubrication of bearings and irrotational fluid flow can be solved when using quasi-harmonic equation. As had been shown by Moaveni (2008) based on time, there are two modes of groundwater flow: steady-state and transient groundwater flow. As had been stated by Bathe (1996) the main characteristic of steady-state problem is that the system response does not change with time. As had been presented by Hinton and Owen (1979) and Wang and Anderson (1982) Galerkin's method and the finite element technique are so frequently combined in computer solution of groundwater flow programs that the two have become particularly synonymous. Galerkin's method is based on a particular principle of weighted residual which is determined directly by governing partial differential equation without need to the physical quantity resort.

Reilly (1984) developed a computer program to evaluate radial flows. Adeboye et al. (2013) presented 2D flow non-homogenous Laplace equation hydorolic conductivity and piezometric head. Kulkani (2018) developed a Eulerian–Lagrangian formulation using numerical models to evaluate groundwater pollution which considered as a challenge of obtaining precise and stable numerical solution. Igboekwe (2014) in his paper finite element method of modeling solute transmit in groundwater flow studied movement of water solute from the surface to aquifer using finite element analysis and reviewed of analytical methods and numerical methods (finite deference and finite element). Jansser and Hemker (2004) presented regional models for large or long-term projects, analytical and numerical models, restrictions of analytical models and advantages of

M. S. Omer (✉)
Roads, Bridges, and Drainage Corporation, Khartoum, Sudan
e-mail: marwasuliman27@gmail.com

A. E. Mohamed
Sudan University of Science and Technology, Khartoum, Sudan

G. H. A. Salih and R. A. Saeed (eds.), *Sustainability Challenges and Delivering Practical Engineering Solutions*,
Advances in Science, Technology & Innovation, https://doi.org/10.1007/978-3-031-26580-8_19

numerical models, and advantages of finite elements with triangular grid. Rouhani (2007) presented a finite element numerical solution for groundwater models discretized by triangular element grid using an object-oriented approach. Kalantari et al. (2018) modeled Birjand aquifer in two dimensions by the isogeometric analysis using four-point Gauss integration method.

In this paper, a numerical solution for finite element is formulated for steady state groundwater flow evaluated by grid of triangular element. Then, a MATLAB program is deveoped for this purpose to get firstly the unknown potential function at the triangular elements nodes. The Simulation of Finite element Field problems MATLAB Program (SFFP) was developed and implemented, as a check and test of nodal potential value.

2 Methodology

In this part, all the indispensable numerical solution and theoretical expressions stages for solution of quasi-harmonic equation are presented. Then, these steps were coded, and the simulation of SFFP was developed and implemented.

The fluid flow through a soil in two dimensions is governed by the equation:

$$\frac{\partial}{\partial x}\left(k_x\frac{\partial \emptyset}{\partial x}\right)+\frac{\partial}{\partial y}\left(k_y\frac{\partial \emptyset}{\partial y}\right)+Q=0 \tag{1}$$

Present the biharmonic equation and its solution.

Where:

$\emptyset \equiv$ The potential function.

$k_x, k_y \equiv$ Permeability coefficients.

The boundary conditions (B.Cs):

(A) Specified at nodal point

$$\emptyset = \emptyset p \tag{2a}$$

(B) Loading boundary

$$k_x\frac{\partial \emptyset}{\partial x}n_x+k_y\frac{\partial \emptyset}{\partial y}n_y+q+\alpha(\emptyset-\emptyset_a)=0 \tag{2b}$$

D.E

$$\frac{\partial}{\partial x}\left(k_x\frac{\partial \emptyset}{\partial x}\right)+\frac{\partial}{\partial y}\left(k_y\frac{\partial \emptyset}{\partial y}\right)+Q=0$$

which is the quasi-harmonic equation with:

$$Q = S-\frac{\mathrm{d}V}{\mathrm{d}t}$$

$$\alpha = q = 0$$

and B.C^s. $\emptyset = \emptyset p = 0$.

$S \equiv$ Rate of fluid injection per unit volume.

$\frac{\mathrm{d}V}{\mathrm{d}t} \equiv$ Rate of volume change per unit volume.

The Galerkin's Method

Employing Galerkin's weighted residual process, assuming a solution $\emptyset$ results in residuals as:

$$e_A=\frac{\partial}{\partial x}\left(k_x\frac{\partial \emptyset}{\partial x}\right)+\frac{\partial}{\partial y}\left(k_y\frac{\partial \emptyset}{\partial y}\right)+Q\neq 0 \tag{3a}$$

From the D.E.

$$e_B=k_x\frac{\partial \emptyset}{\partial x}n_x+k_y\frac{\partial \emptyset}{\partial y}n_y+q+\alpha(\emptyset-\emptyset_a)\neq 0 \tag{3b}$$

From the B.C^s, the weighted residuals:

$\int_A e_A w_A \mathrm{d}A + \int_{SB} e_B w_S \mathrm{d}S = 0$

$$\int_A\left[\frac{\partial}{\partial x}\left(k_x\frac{\partial \emptyset}{\partial x}\right)+\frac{\partial}{\partial y}\left(k_y\frac{\partial \emptyset}{\partial y}\right)+Q\right]w_A\mathrm{d}A + \int_{SB}\left[k_x\frac{\partial \emptyset}{\partial x}n_x+k_y\frac{\partial \emptyset}{\partial y}n_y+q+\alpha(\emptyset-\emptyset_a)\right]w_S\mathrm{d}S=0. \tag{4}$$

Integrating each term by parts, choosing weight $w = w_A = w_S$, and arranging results in week integral form as:

$$-\int_A\left[\frac{\partial w}{\partial x}k_x\frac{\partial \emptyset}{\partial x}+\frac{\partial w}{\partial y}k_y\frac{\partial \emptyset}{\partial y}+wQ\right]\mathrm{d}A + \int_{SA}\left[k_x\frac{\partial \emptyset}{\partial x}n_x+k_y\frac{\partial \emptyset}{\partial y}n_y\right]w\mathrm{d}S-\int_{SB}[q+\alpha(\emptyset-\emptyset_a)]w\mathrm{d}S=0 \tag{5}$$

Finite Element Representation of Weak Form

Approximately, the function $\emptyset$ and weight using shape function N_i for a finite element discretization with n nodes substituting in week form gives:

$$-\int_A\left[\left(\frac{\partial N_i}{\partial x}k_x\frac{\partial N_j}{\partial x}+\frac{\partial N_i}{\partial y}k_y\frac{\partial N_j}{\partial y}\right)\emptyset_j-N_iQ\right]\mathrm{d}A+x_i - \int_{SB}N_i\left[q-\alpha\emptyset_a+\alpha\sum_{j=1}^{n}N_j\emptyset_j\right]\mathrm{d}S=0 \tag{6}$$

Rearranging gives:

$$\left[\int_A \sum_{j=1}\left(\frac{\partial N_i}{\partial x}k_x\frac{\partial N_j}{\partial x}+\frac{\partial N_i}{\partial y}k_y\frac{\partial N_j}{\partial y}\right)\mathrm{d}A+\alpha\sum_{j=1}^{n}N_j\emptyset_j\right]\emptyset_j = \int_A N_i Q\mathrm{d}A-\int_{SB}N_i[q-\alpha\emptyset_a+]\mathrm{d}S+x_i \tag{7}$$

$$i,j \equiv \text{from 1 to } n$$

In which:

$$x_i=\sum_{j=1}\int_{SB}\left[k_x\frac{\partial N_j}{\partial x}n_x+k_y\frac{\partial N_j}{\partial y}n_y\right]\emptyset_j N_i\mathrm{d}S$$

That represents constrains (reactions).
Equation (7) can be written as:
OR:

$$\{k^e\}\{\emptyset^e\}=\{f^e\} \tag{8}$$

where:
The element stiffness matrix is:

$$\{k^e\}=\int_A\sum_{j=1}\left(\frac{\partial N_i}{\partial x}k_x\frac{\partial N_j}{\partial x}+\frac{\partial N_i}{\partial y}k_y\frac{\partial N_j}{\partial y}\right)dA+\alpha\sum_{j=1}^{n}N_j\emptyset_j \tag{9a}$$

The element nodal load vector is:

$$\{f^e\}=\int_A N_i Q\mathrm{d}A-\int_{SB}N_i[q-\alpha\emptyset_a+]\mathrm{d}S+x_i \tag{9b}$$

Evaluation of the Triangular Element Properties

Finite element grid using simple triangular element (Fig. 1) is convenient to approximate arbitrary-shaped regions with small deviations. Based on Eq. (8), the triangular element is formulated as follows:

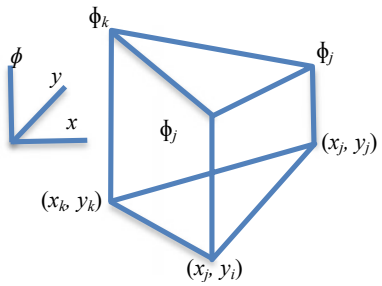

Fig. 1 Nodal values of the potential function for a triangular element

- The potential function within any point at triangle is given in terms of the shape functions and nodal potential values as follows:

$$\{\emptyset^e\}=\sum_{i=1}^{3}N_i\emptyset_i^e=\{N_1N_2N_3\}\{\emptyset_1^e\emptyset_2^e\emptyset_3^e\} \tag{10}$$

where the shape functions N_1, N_2 and N_3 are:

$$\begin{aligned}N_1&=\frac{1}{2A}(a_1+b_1x+c_1y)\\ N_2&=\frac{1}{2A}(a_2+b_2x+c_2y)\\ N_3&=\frac{1}{2A}(a_3+b_3x+c_3y)\end{aligned} \tag{11}$$

and A is the element area.

- The element stiffness matrix is then given from Eqs. (9a), (10), and (11) by:

$$\{k^e\}=\{k^e\}_I+\{k^e\}_{12}+\{k^e\}_{23}+\{k^e\}_{31} \tag{12}$$

In which:

$$\begin{aligned}\{k^e\}_I&=\sum_{i=1}^{n}\sum_{j=1}^{n}\frac{1}{4A}\left(k_xb_ib_j+k_yc_ic_j\right)\\ &=\frac{k_x}{4A}\{b_1b_1b_1b_2b_1b_3b_2b_1b_2b_2b_2b_3b_3b_1b_3b_2b_3b_3\}\\ &\quad+\frac{k_y}{4A}\{c_1c_1c_1c_2c_1c_3c_2c_1c_2c_2c_2c_3c_3c_1c_3c_2c_3c_3\}\end{aligned} \tag{13}$$

and

$$\{k^e\}_{12}=\frac{\alpha S_{12}^e}{6}\{210120000\} \tag{14a}$$

$$\{k^e\}_{23}=\frac{\alpha S_{23}^e}{6}\{000021012\} \tag{14b}$$

$$\{k^e\}_{31}=\frac{\alpha S_{12}^e}{6}\{201000102\} \tag{14c}$$

- Element nodal load vector, neglecting x_i, is given from (9b) and (11) as:

$$\{f^e\}=\{f^e\}_Q+\{f^e\}_{c12}+\{f^e\}_{c23}+\{f^e\}_{c31} \tag{15}$$

where:

$$\{f^e\}_Q = \frac{QA}{3}\{111\} \tag{16a}$$

$$\{f^e\}_{c12} = -\frac{(q-\alpha\emptyset_a)S^e_{12}}{2}\{110\} \tag{16b}$$

$$\{f^e\}_{c23} = -\frac{(q-\alpha\emptyset_a)S^e_{23}}{2}\{011\} \tag{16c}$$

$$\{f^e\}_{c31} = -\frac{(q-\alpha\emptyset_a)S^e_{31}}{2}\{101\} \tag{16d}$$

Groundwater flow:

The fluid flow:

$$\frac{\partial}{\partial x}\left(k_x\frac{\partial h}{\partial x}\right)+\frac{\partial}{\partial y}\left(k_y\frac{\partial h}{\partial y}\right)+Q=0 \tag{17}$$

$h \equiv$ Pressure head.

In case of steady-state groundwater flow:

$$Q = S - \frac{\mathrm{d}V}{\mathrm{d}t} \tag{18}$$

$$\alpha = q = 0$$

Based on the above formulation and B.Cs, an adopted modular process with a separate subroutine will be utilized to perform the main operation. These subroutines are then called in sequence by a main or master program.

3 Results

The program SFFP was applied for solution of a two-dimensional porous medium problem, fluid flow problem, and body exposure to a heat source problem. In the meantime, the results obtained were compared with published data as follows:

3.1 Case One: Two-Dimensional Porous Medium

Sandy soil region with two-dimensional shown in the adapted Fig. 2 (Logan 2007), it is required to measure the potential distribution. The tension (fluid head) on the left part is a constant equal to 10.0m, and that on the right part is 0.0. The upper and lower sides are impervious. The impervious are $k_{xx} = k_{yy} = 25 \times 10^{-5}\frac{m}{s}$. Unit thickness is assumed. The results obtained using SFFP are presented in Table 1 and compared with solution presented by Logan (2007).

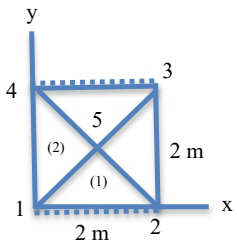

Fig. 2 Two-dimensional porous medium

As can be seen from Table 1, the nodal potential obtained using SFFP completely agrees with the known published result with no difference.

3.2 Case Two: Two-Dimensional Fluid Flow Problem

The fluid flow problem shown discretized in Fig. 3—which is adapted from Logan (2007)—has the top and bottom parts impervious, whereas the right side has a constant head of 3cm and the left side has a constant head of 4cm. The nodal potential result obtained using SFFP is presented in Table 2 and compared with solution presented by Logan (2007).

The compression shows complete agreement between the two results.

As can be seen from Table 2, the result obtained using SFFP completely agrees with the known published result with no difference.

Table 1 Two-dimensional porous medium results

Node number	Nodal potential value(cm)		Difference %
	Logan (2007)	SFFP solution	
1	10.0000	10.0000	0.00
2	0.0000	0.0000	0.00
3	0.0000	0.0000	0.00
4	10.0000	10.0000	0.00
5	5.0000	5.0000	0.00

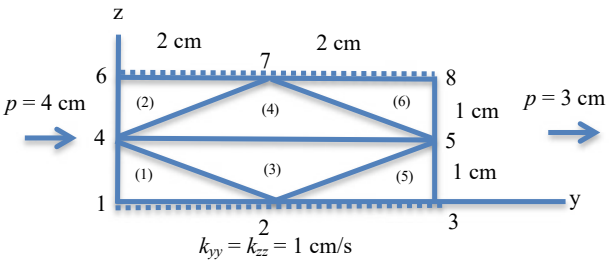

Fig. 3 Two-dimensional fluid flow problem

Table 2 Two-dimensional fluid flow problem results

Node number	Nodal potential values (cm)		Difference %
	Logan (2007)	SFFP solution	
1	4.0000	4.0000	0.00
2	3.5000	3.5000	0.00
3	3.0000	3.0000	0.00
4	4.0000	4.0000	0.00
5	3.0000	3.0000	0.00
6	4.0000	4.0000	0.00
7	3.5000	3.5000	0.00
8	3.0000	3.0000	0.00

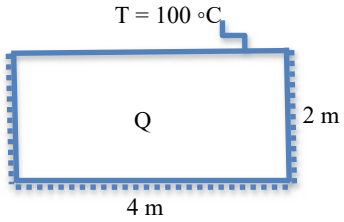

Fig. 4 Two-dimensional body subjected to a heat source

3.3 Case Three: Body with Two-Dimensional Exposure to a Heat Source

For the body with two-dimensional shown in in the adapted Fig. 4 (Logan 2007), it is required to measure the distribution of temperature. The temperature of the upper part of the body is maintained at 100 °C. The body is isolated on the other sides. A uniform heat source of Q = 1000 $\frac{W}{m^3}$ acts over the whole plate, as shown in the figure. A constant thickness of 1 m is assumed. Let $k_{xx} = k_{yy} = 25$ W/(m °C).

We need attention just for the left half of the body, because we have a vertical plane of the symmetry passing through the body 2 m from both the left and right portions. This vertical plane can be considered as isolated boundary. The finite element model is shown in the adapted Fig. 5 (Logan 2007). The results obtained using SFFP are presented in Table 3 and compared with solution presented by Logan (2007).

Fig. 5 Discretized body of Fig. 4

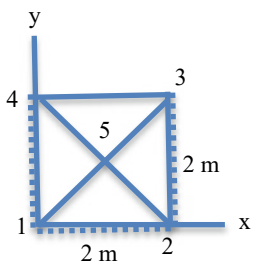

Table 3 Body with two-dimensional exposure to a heat source results

Node number	Nodal temperature values (°C)		Difference %
	Logan (2007)	SFFP solution	
1	180.0000	180.0000	0.00
2	180.0000	180.0000	0.00
3	100.0000	100.0000	0.00
4	100.0000	100.0000	0.00
5	153.0000	153.3333	0.22

As can be seen from Table 3, the result obtained using SFFP closely agrees with the known published result with a maximum percentage difference of 0.22%.

4 Discussion

This case study focused on the flow of groundwater beneath a coffer dam which had been solved by using a potential formulation as done by Hinton and Owen (1979). The geometry of the model is evident in Fig. 6 (Hinton and Owen 1979). It is supposed that boundary ABC is impervious (no leakage) as is the sheet pile wall EFG. The pressure head in this case is the difference in height between AG and DF which is 3 units. Arbitrarily setting $\emptyset = 0.0$ along DF, since the flow speeds depend only on the gradient of $\emptyset$, then $\emptyset = 3.0$ along AG. Along ABC and on either side of the sheet pile wall, it is required that $\frac{\partial \emptyset}{\partial n} = 0$ also symmetry conditions along CD require $\frac{\partial \emptyset}{\partial n} = 0$ on this part. These boundary conditions are shown in Fig. 6. The equi-potential lines obtained by Hinton and Owen (1979) are also shown in the same figure.

The finite element mesh employed for the case study using SFFP is illustrated in Fig. 7. Figure 8 presents the equi-potential lines obtained using SFFP.

Referring to Figs. 6 and 8, the results show very close agreement. To confirm this, the values of nodal potential of five randomly selected nodes are presented and compared with the solution presented by Hinton and Owen (1979) in Table 4.

Results shown in Table 4 are in very close agreement with a maximum percentage difference of 1.32% (mainly due to the interpolation of the reference results). If SFFP results are approximated to two decimals as those of the reference, the results are almost identical (maximum percentage difference = 0.36%). This verifies the accuracy SFFP results.

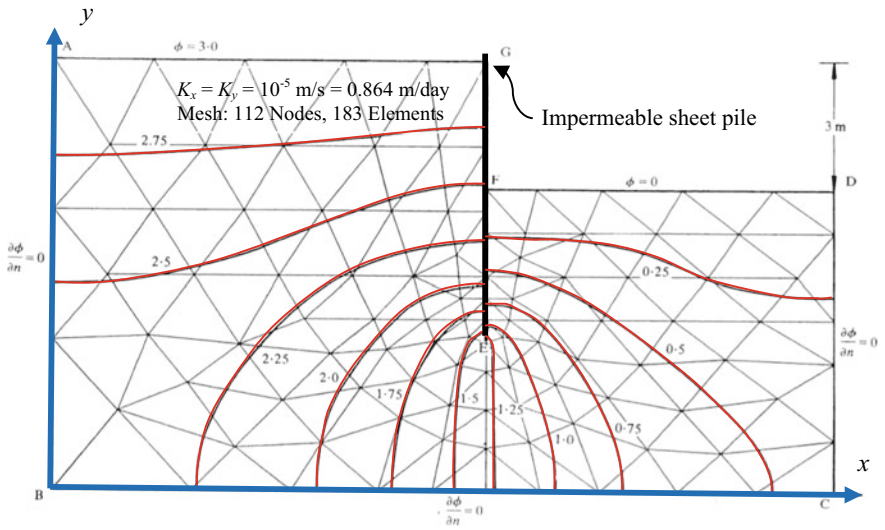

Fig. 6 Groundwater flow beneath a coffer dam showing equi-potential lines

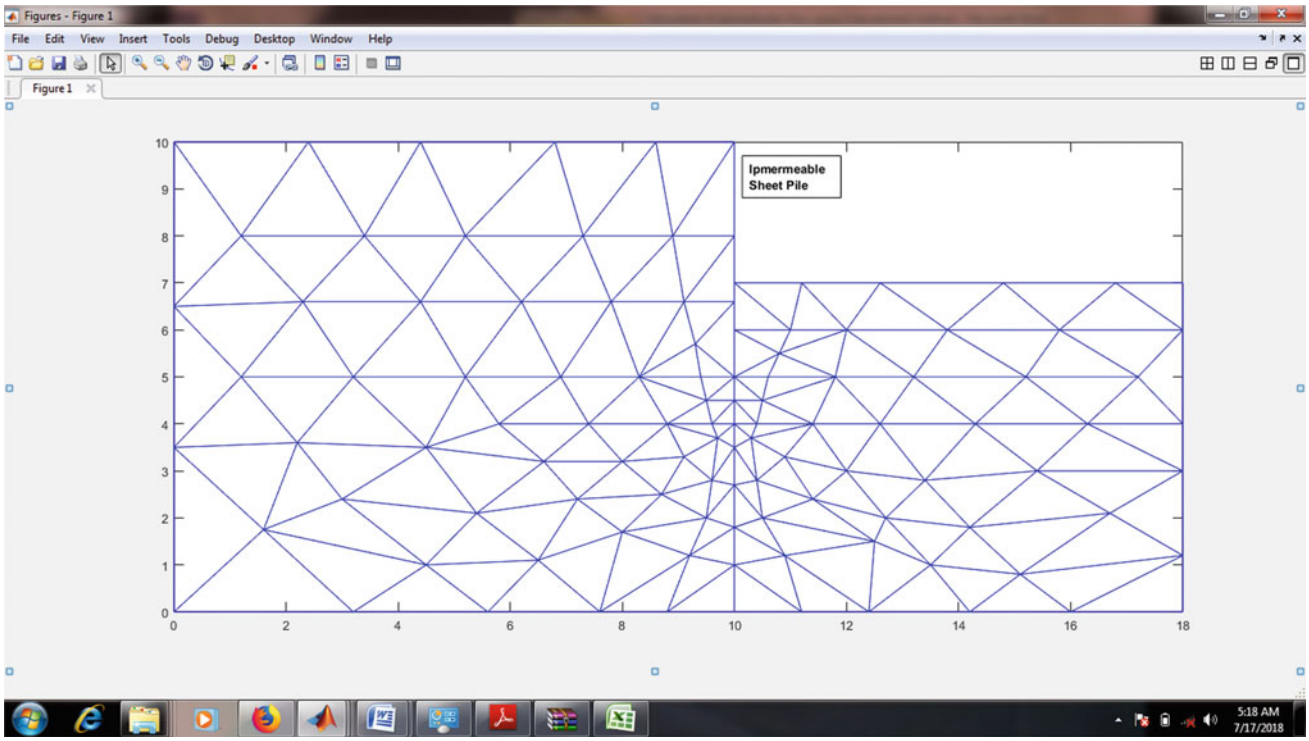

Fig. 7 Finite element mesh employed for the case study using SFFP

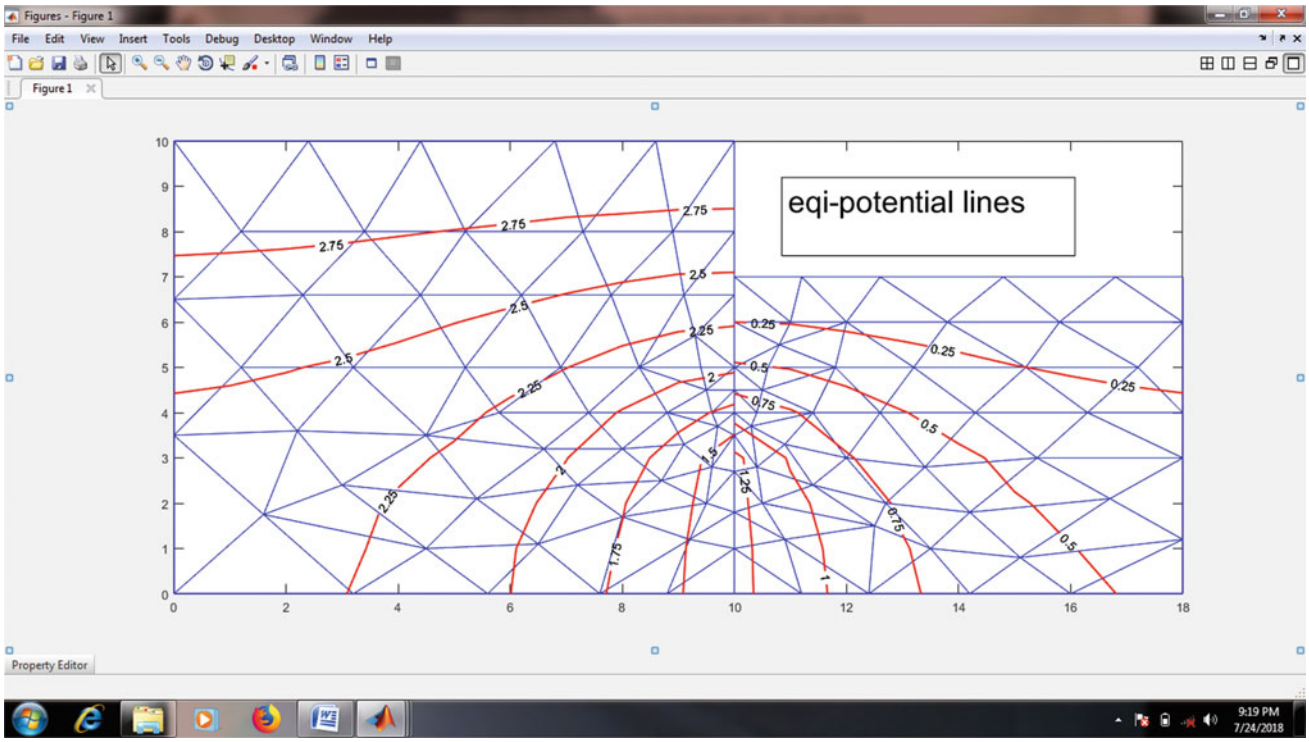

Fig. 8 Groundwater flow beneath a coffer dam showing equi-potential lines obtained using SFFP

Table 4 Comparison between SFFP and Hinton and Owen (1979) Nodal potential values

Node Number	Nodal potential values (m)		Difference %
	Hinton and Owen (1979)	SFFP solution	
11	2.25	2.2505	00.02
22	2.75	2.7417	−00.30
33	1.75	1.7473	−00.15
65	0.53	0.5307	00.13
99	0.25	0.2467	−01.32

5 Conclusions

From the result presented in this paper, the finite element solution of quasi-harmonic equation was formulated for steady-state groundwater flow. Then MATLAB was used to develop SFFP for solution of quasi-harmonic equation. SFFP was implemented, and its results accuracy verified by comparing with known results. The comparison showed very close agreement between results with a maximum difference of 0.22%. SFFP program was applied to a groundwater flow beneath a coffer dam problem as a case study. The results obtained using SFFP were in close agreement with the published results with a maximum difference of 1.32%.

References

K.R. Adeboye, M.D. Shehu, A. Ndanusa, *Finite Element Discretization and Simulation of Ground Water Flow System, IOSR-JM*, vol. 5, issue 6, pp. 54–61 (2013)

K.J.F. Bathe, *Finite Element Procedures* (Prentice Hall, New Jersey, 1996)

E. Hinton, D.R.J. Owen, *An introduction to finite element computational procedures*. Great Britain, Redwood Burn (1979)

M.U. Igboekwe, *Finite Element Method of Modeling Solute Transport in Groundwater Flow, PJST*, vol. 15

G. Jansser, K. Hemker, *Groundwater Models as Civil Engineering Tools*, FEM-MODFLOW, Czech Republic (2004)

M. Kalantari, A. Akbarpour, M. Khatibinia, Numerical modeling of groundwater flow in unconfined aquifer in steady state with isogeometric method. Modares Civil Eng. J. (M.C.E.J) **18**(3), 195–206 (Persian, 2018)

N.H. Kulkarni, A new numerical model coupling modified method of characteristics and garkin finite element method for simulation of solute transport in groundwater flow system. AQUADEMIA Water Environ. Technol. (2018)

D.L. Logan, *A first Course in The Finite Element*, United States, Chris Carson (2007)

S. Moaveni, *Finite Element Analysis: Theory and Application with ANSYS*, 3rd edn (Pearson Prentice Hall, United States of America, 2008)

T.E. Reilly, *A Galerkin's Finite Element Flow Model to Predict the Transient Response of a Radially Symmetric Aquifer*. U.S. Geological Survey Water Supply Paper2198 (1984)

A.L.K. Rouhani, 2D modeling of groundwater flow using finite element method in an object-oriented approach, in *IMWA Symposium, Water in Mining Environment*, Italy (2007)

H.F. Wang, M.P. Anderson, *Introduction to Groundwater Flow Modeling: Finite Difference and Finite Element Method*, San Francisco (1982)

O.C. Zienkiewicz, R.L. Taylor, J.Z. Zhu, *A Multidimensional Finite Element Method* (Butterworth-Heinemann, Amsterdam, Boston, 2013)